PSTP15: Design of the of the Mainz

Active Polarized Proton Target

M. Biroth, P. Achenbach, E. Downie, A. Thomas
Institut für Kernphysik, Mainz, Germany

A2

Crystal Ball Collaboration

mami MAINZER MIKROTRON

SFB 1044 THE LOW-ENERGY FRONTIER OF THE STANDARD MODEL

JG|U JOHANNES GUTENBERG UNIVERSITÄT MAINZ

Experimental Setup

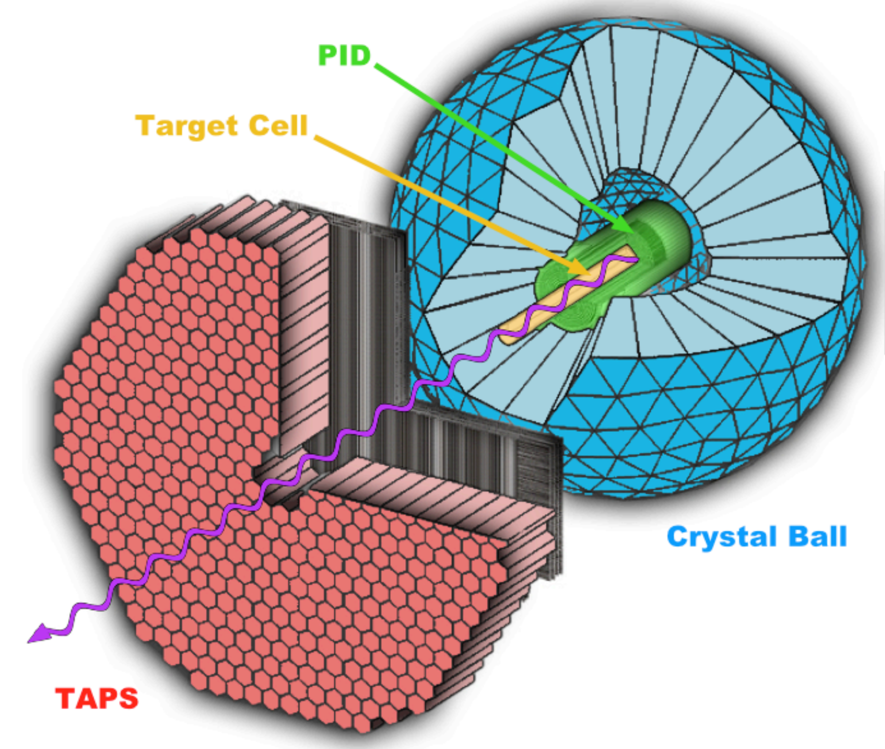

Polarized photon beam

Tagged photons up to 1.6GeV
Circular and linear polarization

4π-Detector

Crystal Ball with 672 NaI crystals

Mainz Frozen Spin Target

^3He-^4He-Dilution cryostat at 25mK
DNP with superconductive Magnet 2.5T, 5T
Internal holding coils 0.68T (L), 0.5T (T) and NMR system

Standard Material H-Butanol

Degree of p-polarization ≈ 85%
Relaxation time more than 2000h

Maik Biroth, Institut für Kernphysik, Mainz, Germany biroth@kph.uni-mainz.de

Motivation for an Active Polarized Proton Target

Double-polarization experiments at the pion threshold

➔ Protons and charged pions get stopped by thermal shielding of cryostat and holding coil

- Real Compton Scattering

  Measuring the spin polarizabilities

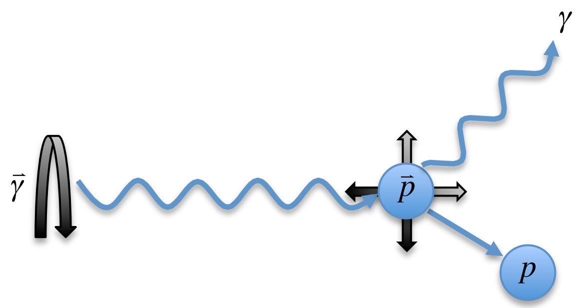

Detecting the recoil proton

➔ Suppress π^0p events

➔ Suppress coherent scattering on heavy nuklei

- Pion production

  Verifying the Gerasimov-Drell-Hearn (GDH) Sum Rule

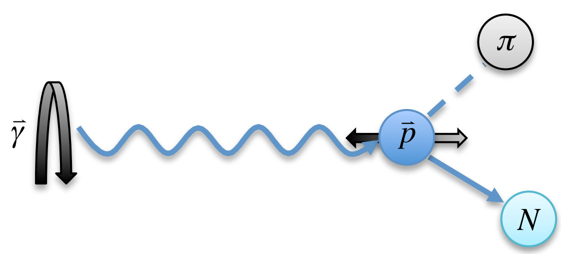

Detecting the π^+

➔ Identify reaction channel π^+n or π^0p

Maik Biroth, Institut für Kernphysik, Mainz, Germany   biroth@kph.uni-mainz.de

Challenges for an Active Polarized Proton Target

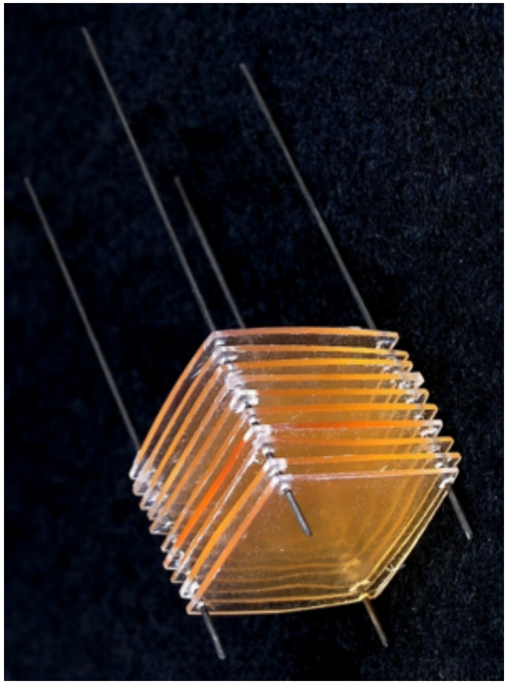

D. Von Maluski et al. Polarizable Scintillator for Nuclear Targets. Technical report, Triangle Universities Nuclear Laboratory (TUNL), 2009

Requirements

- polarizable scintillator
- high rate capability
- high light output
- low thermal energy input
- detectors working @ 4 K

Vehicle	Polystyrene	C_8H_8
Scintillator 365 nm	2,5-Diphenyloxazole PPO	$C_{15}H_{11}NO$
Wavelength Shifter 430 nm	Dimethyl-POPOP	$C_{26}H_{20}N_2O_2$
Paramagnetic Free Radical	4-Oxo-TEMPO	$C_9H_{16}NO_2$

70% polarization @ 200 mK in Mainz

Dilution factor f_p = 7.7% (H-Butanol 13.4%)

Construction of APPT Prototypes

- Design studies standard plastic scintillator
- First beam test results at room temperature
- Increasing the light output
- Modifications for LHe temperatures

Prototypes with Wavelength-Shifting Fibers

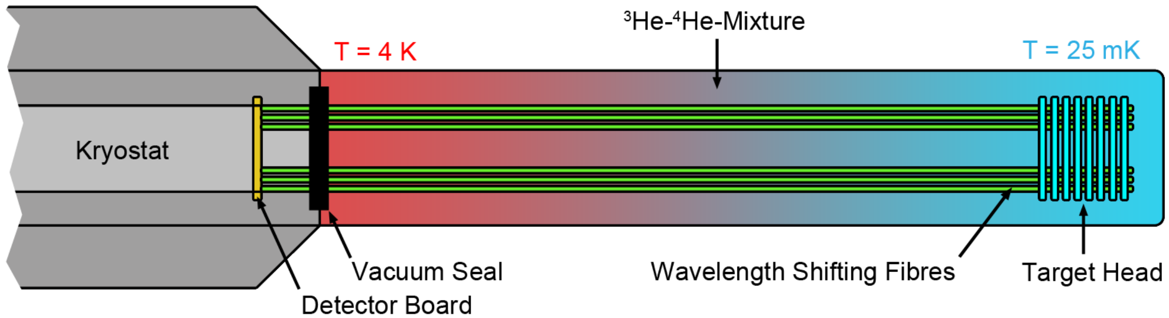

Ø1mm WLS fibers

1mm scintillator slices

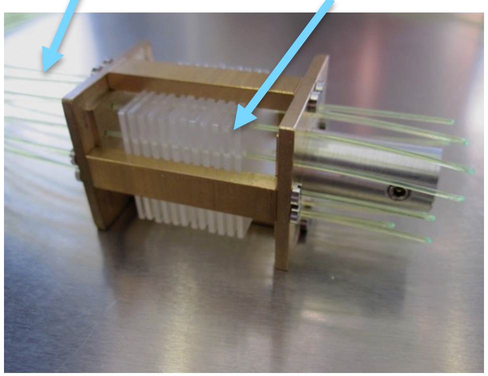

Bad coupling

Ø1.5mm WLS fibers

10mm scintillator block

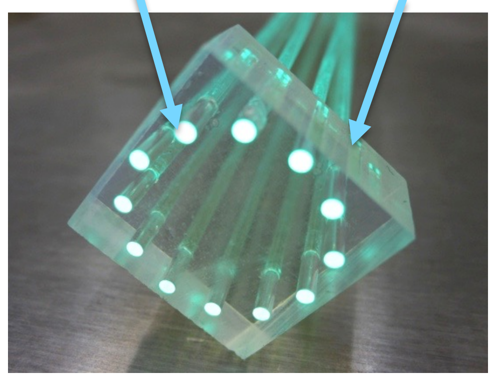

Bad cooling

Ø1.5mm WLS fibers

scintillator layers with cooling holes

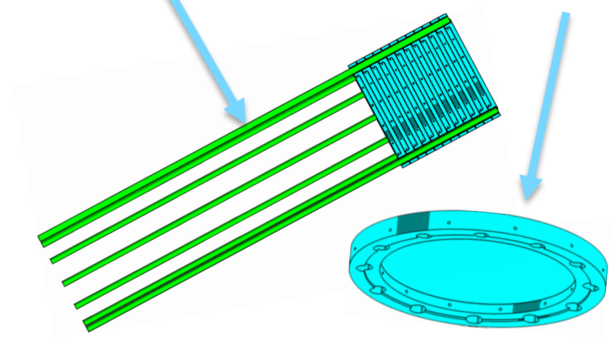

Unrealized design concept

Evolution of prototypes with WLS fibers

Maik Biroth, Institut für Kernphysik, Mainz, Germany

biroth@kph.uni-mainz.de

2 Prototypes with Wavelength-Shifting Head

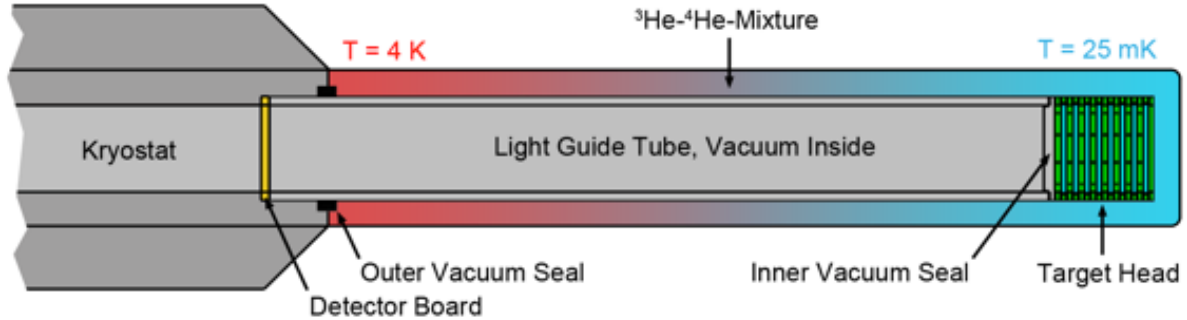

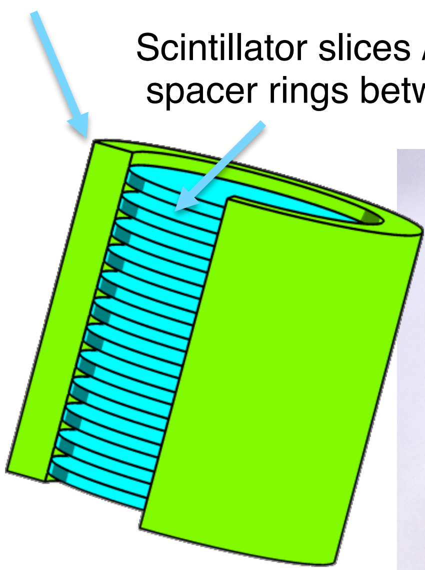

Solid Head

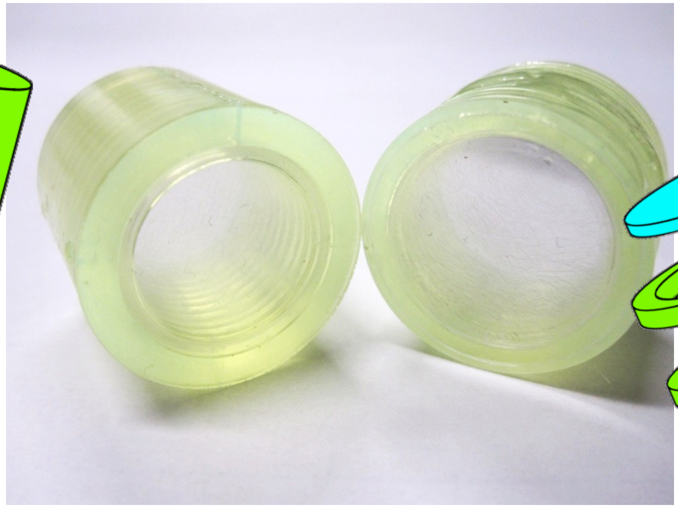

Segmented Head

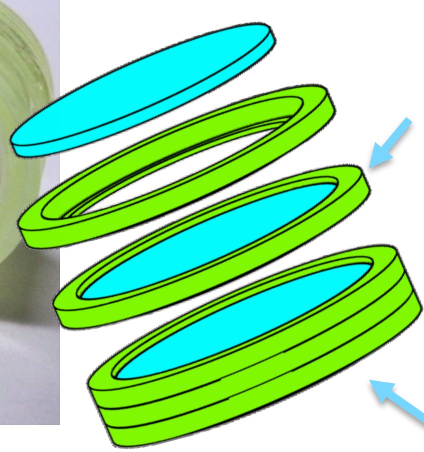

Maik Biroth, Institut für Kernphysik, Mainz, Germany biroth@kph.uni-mainz.de

Components of the Prototypes with Wavelength-Shifting Head

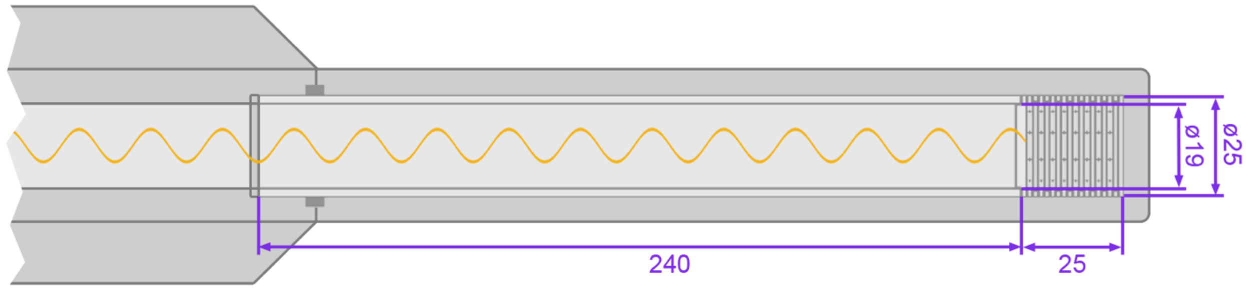

- Standard plastic scintillator BC-408 1 mm
- WLS material BC499-53 25 mm and 2 mm
- Acrylic glass tube with wall thickness of 3 mm

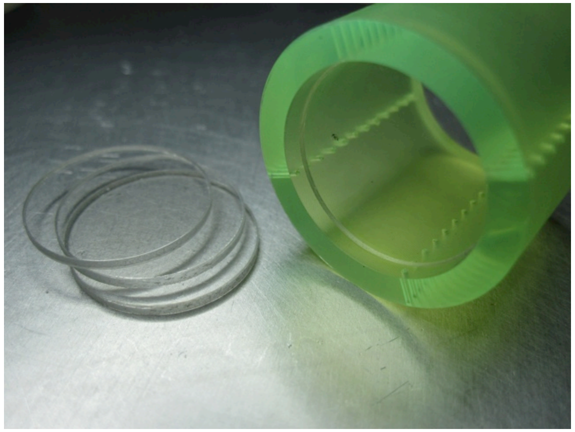

biroth@kph.uni-mainz.de

Manufacturing of the Solid Prototype

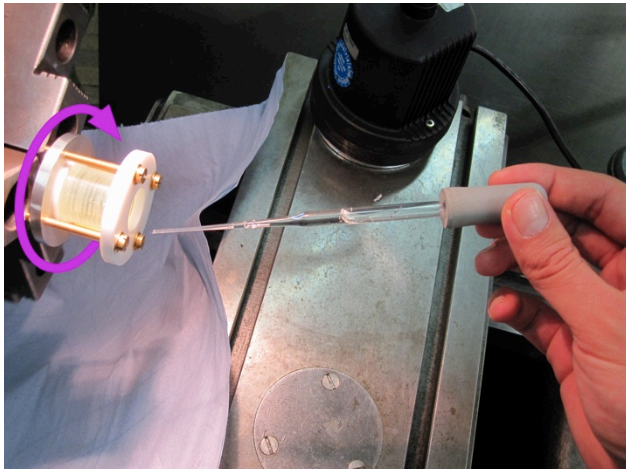

Feeding epoxy while rotating the WLS head

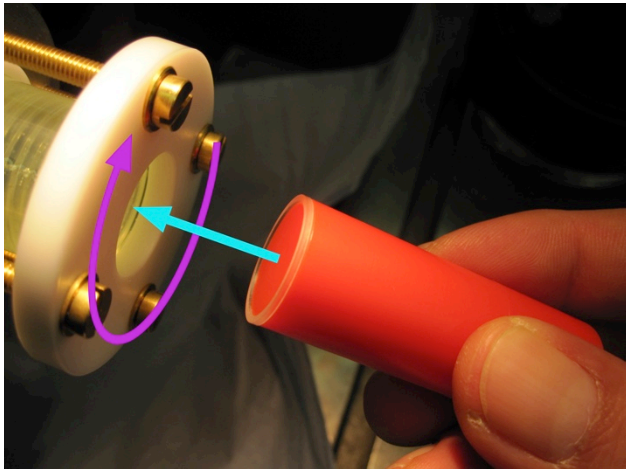

Placing the pieces under rotation

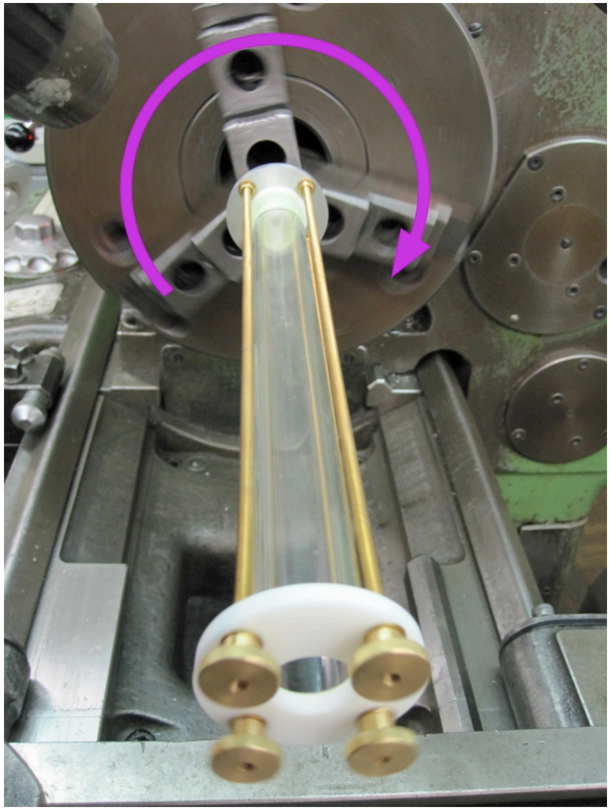

After curing connect the light guide

Maik Biroth, Institut für Kernphysik, Mainz, Germany biroth@kph.uni-mainz.de

Manufacturing of the Segmented Prototype

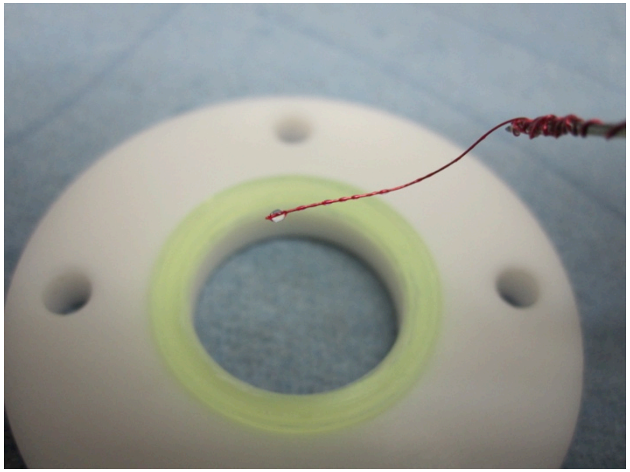

Gluing of the single layers

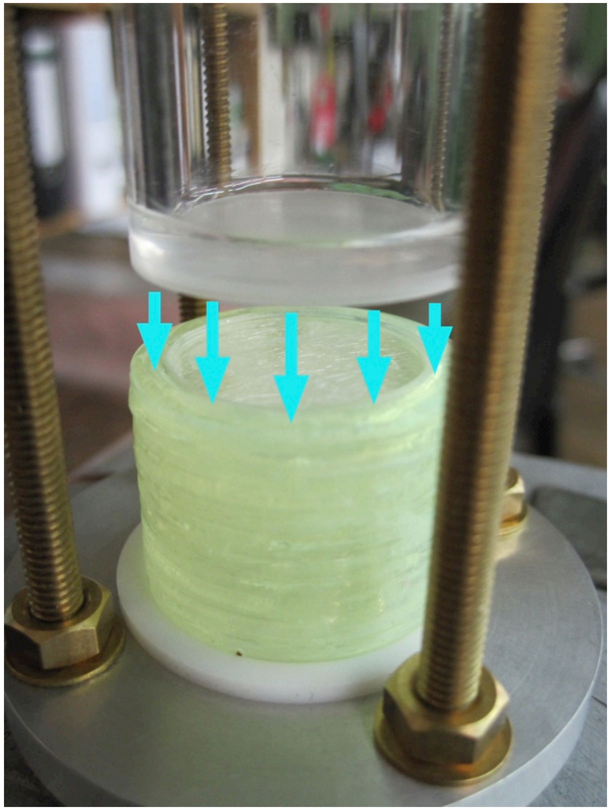

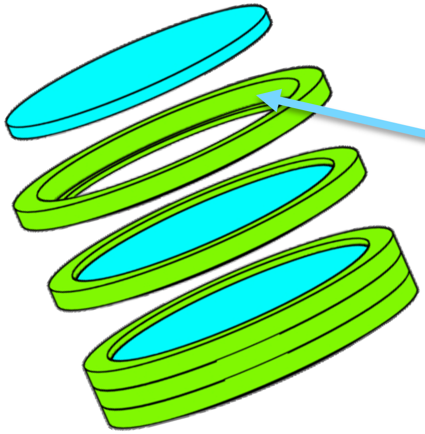

+200% increased
optical contact area

- more adhesive surfaces

Stacking the layers and connecting the light guide

Maik Biroth, Institut für Kernphysik, Mainz, Germany biroth@kph.uni-mainz.de

Setup for a First Beam Test

Detector board with 2 SiPMs and 2 APDs mounted (beam input)

Head of the solid prototype (beam output)

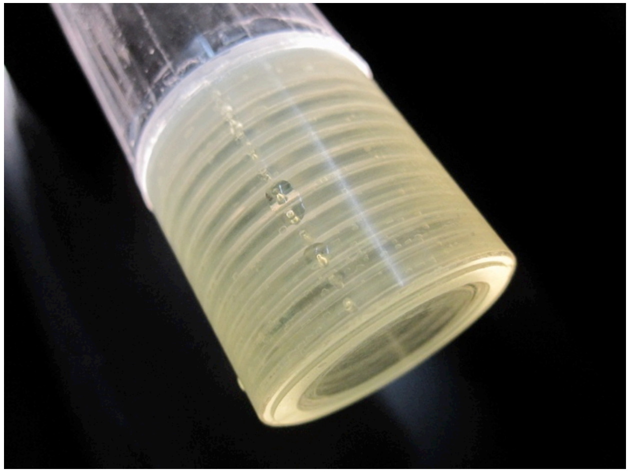

Light tight case with the solid prototype and detector board connected

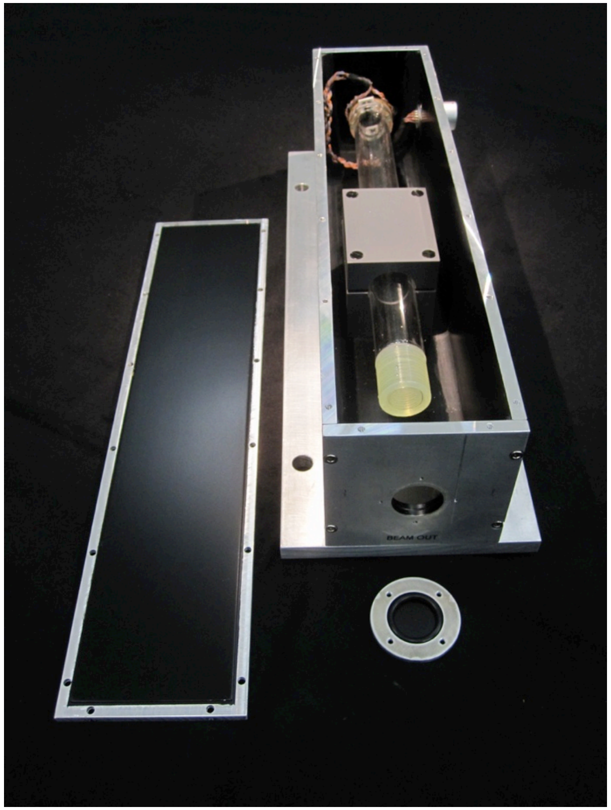

Independent Trigger Logic

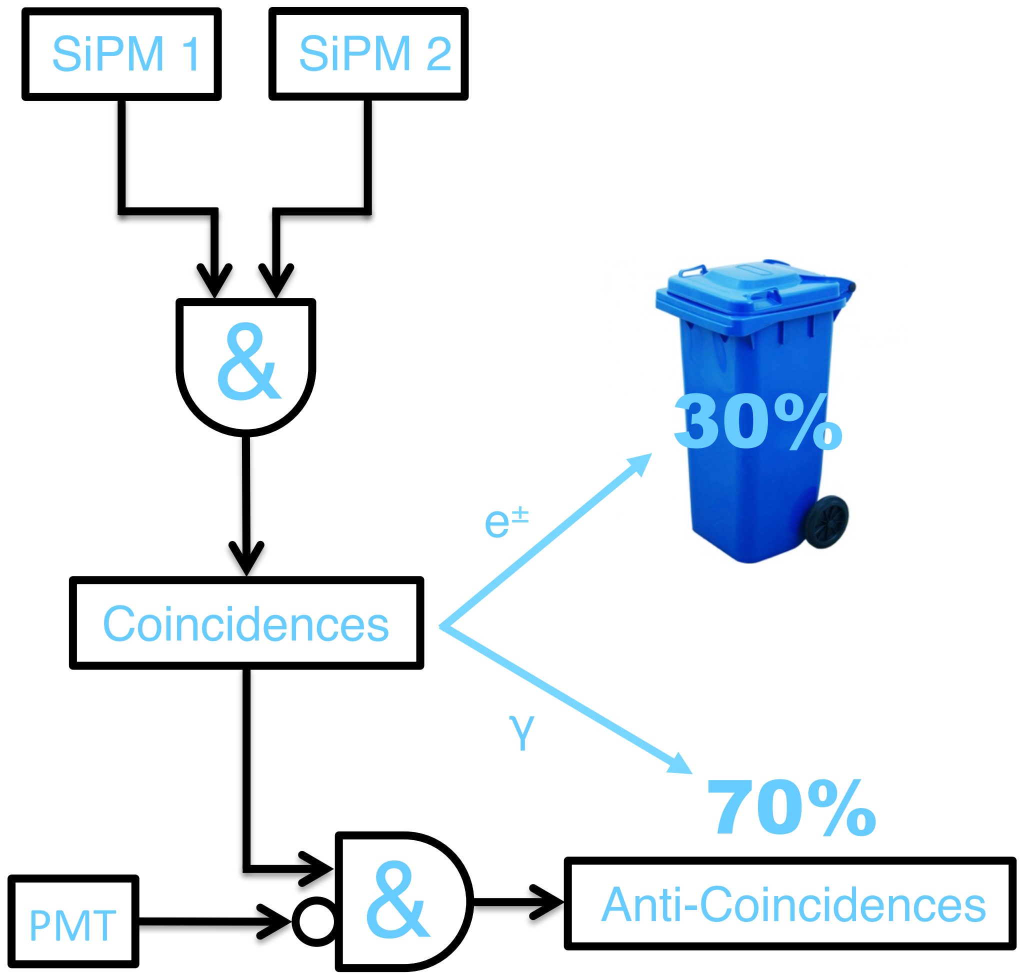

Maik Biroth, Institut für Kernphysik, Mainz, Germany
biroth@kph.uni-mainz.de

Proof of Count Rate Capability

Up to 10 nA of beam current with copper radiator

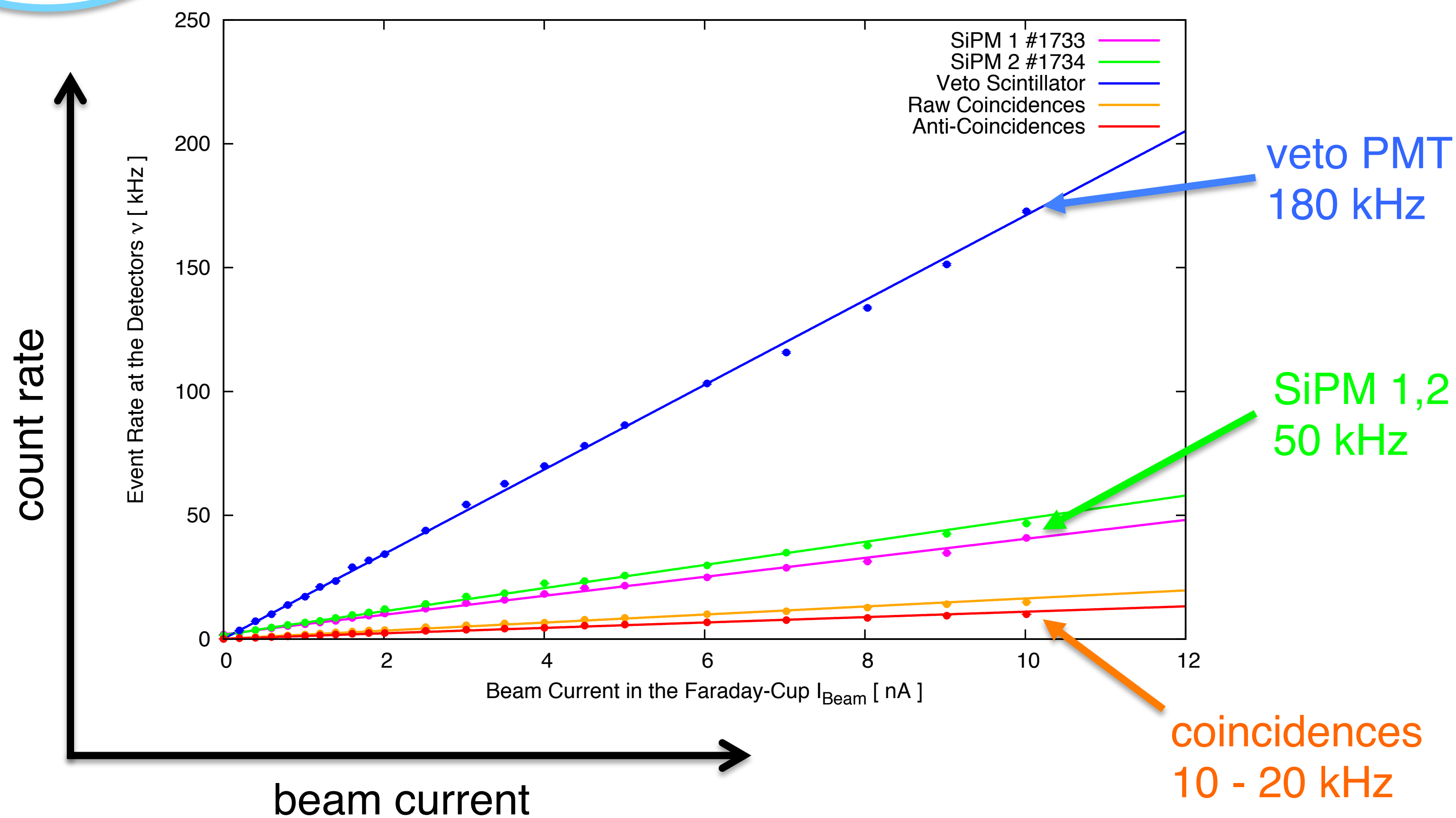

Maik Biroth, Institut für Kernphysik, Mainz, Germany
biroth@kph.uni-mainz.de

Exemplary Beam Test Spectrum
Coherent Edge E_γ = 350 MeV

anti-coincident events ($\gamma \rightarrow e^\pm$, $\gamma + p \rightarrow p + \pi^0$, …)

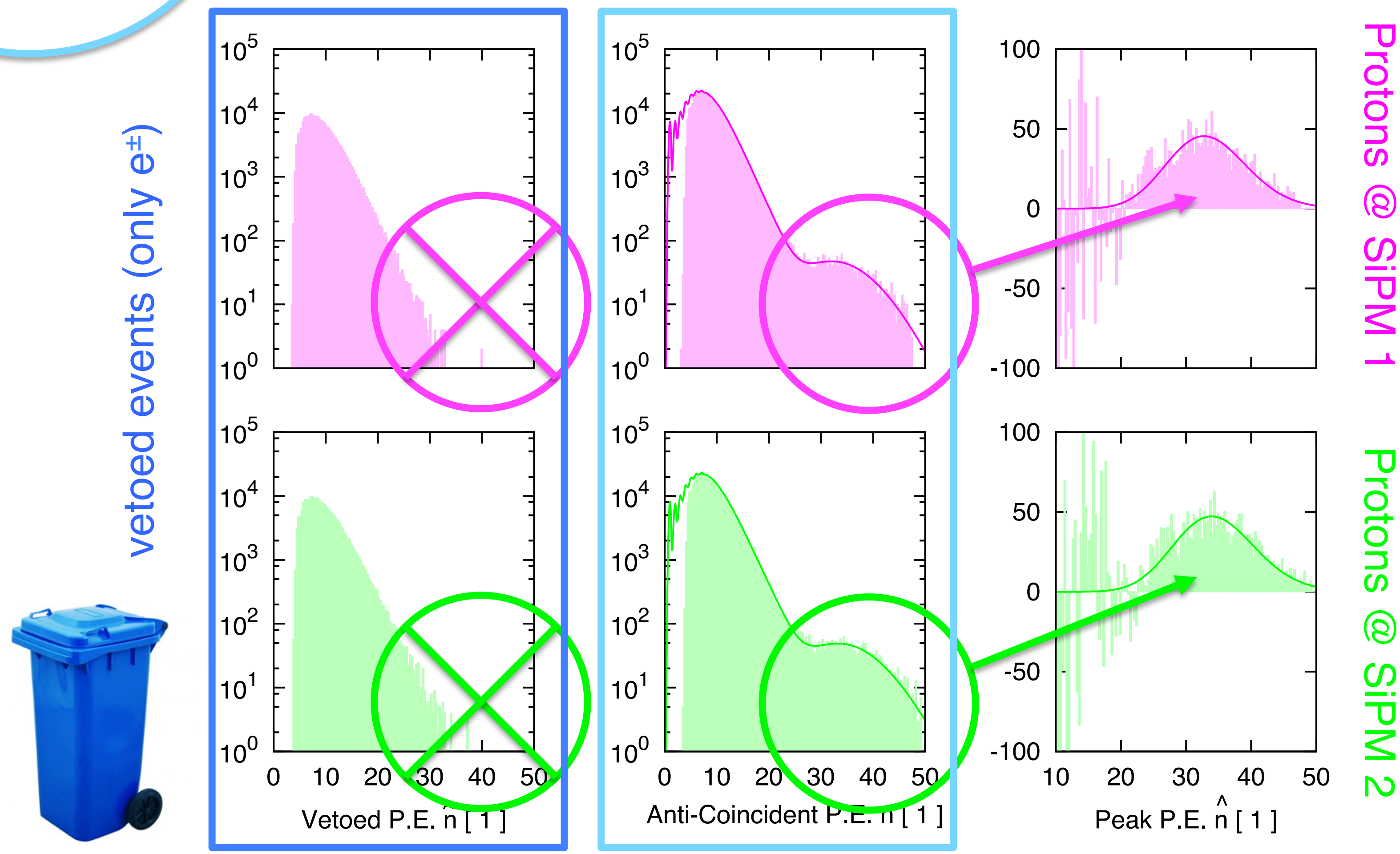

Maik Biroth, Institut für Kernphysik, Mainz, Germany
biroth@kph.uni-mainz.de

Results of the Beam Test

At room temperature electromagnetics and protons were separated by a factor of 5 in energy deposition

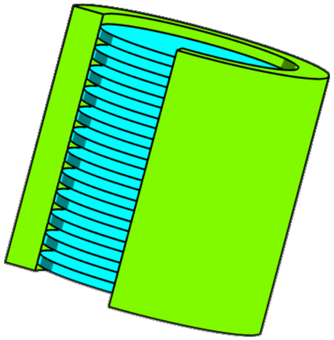

Prototype	Electrons / Positrons	Protons
Solid	1.0 γ mm^{-2}	5.5 γ mm^{-2}
Segmented	0.8 γ mm^{-2}	4.5 γ mm^{-2}

+ 20% – 25% light output

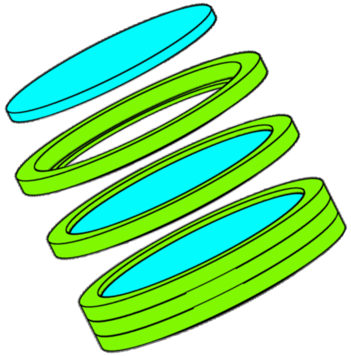

total coupling surface: 200 mm^2

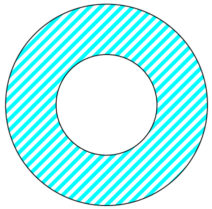

Maik Biroth, Institut für Kernphysik, Mainz, Germany

biroth@kph.uni-mainz.de

Increasing the Light Output by Surface Coating of Scintillator

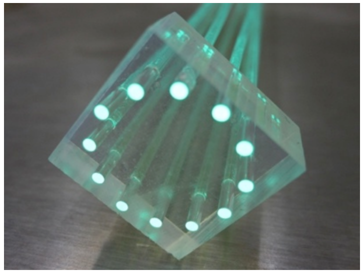

Count rates of 22.2 MBq ^{90}Sr source
All 12 fibers bended to a PMT
Applied Al and PTFE Coatings

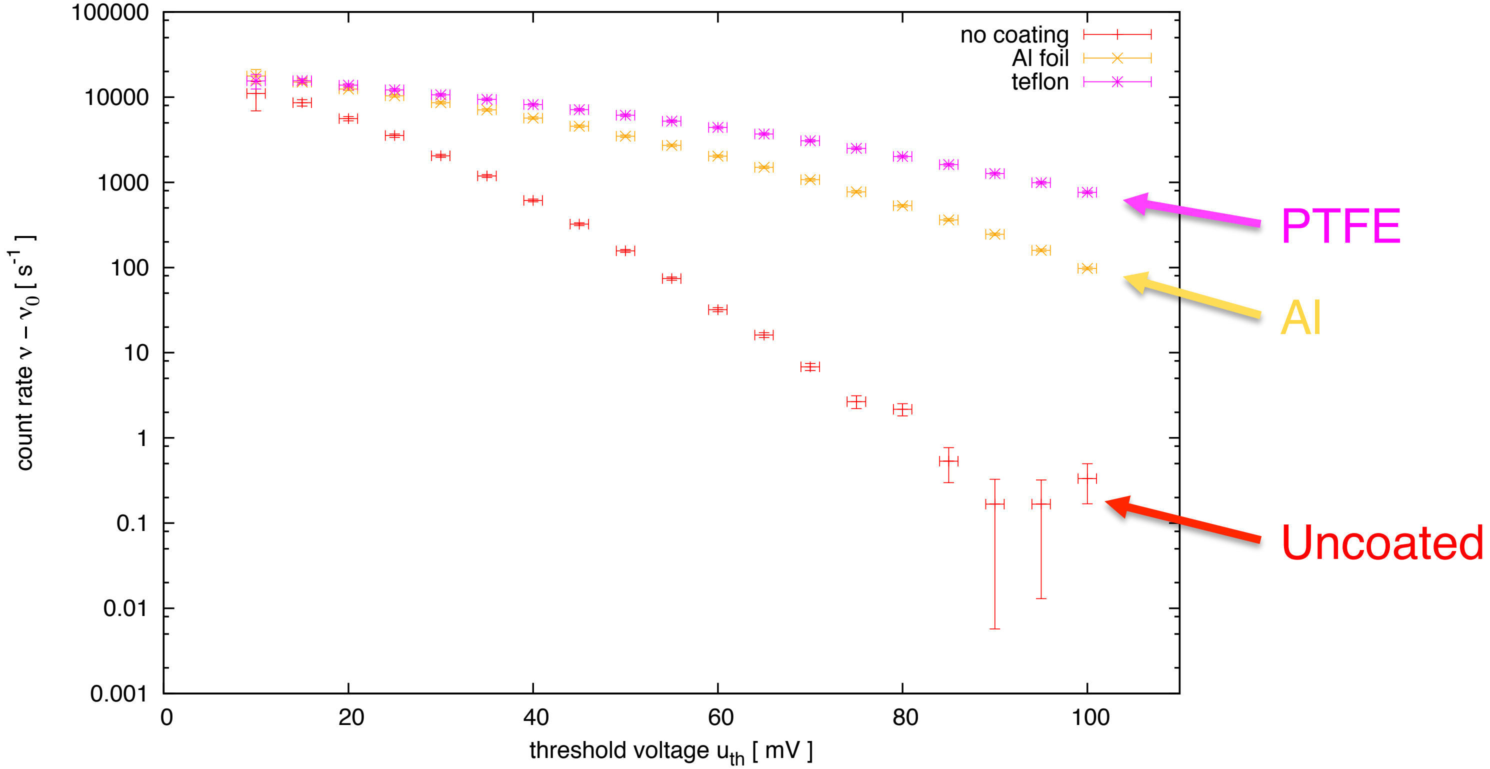

Increasing the Light Output by Coating the WLS Head

2 kinds of total reflection

- Specular reflection
  on smooth surfaces
  like Al foil

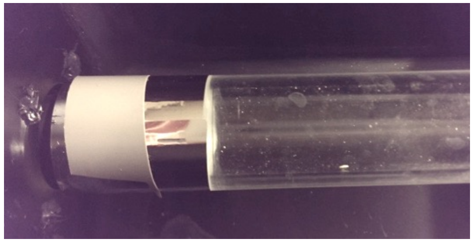

- Diffuse reflection
  on rough surfaces like
  Teflon tape (PTFE)

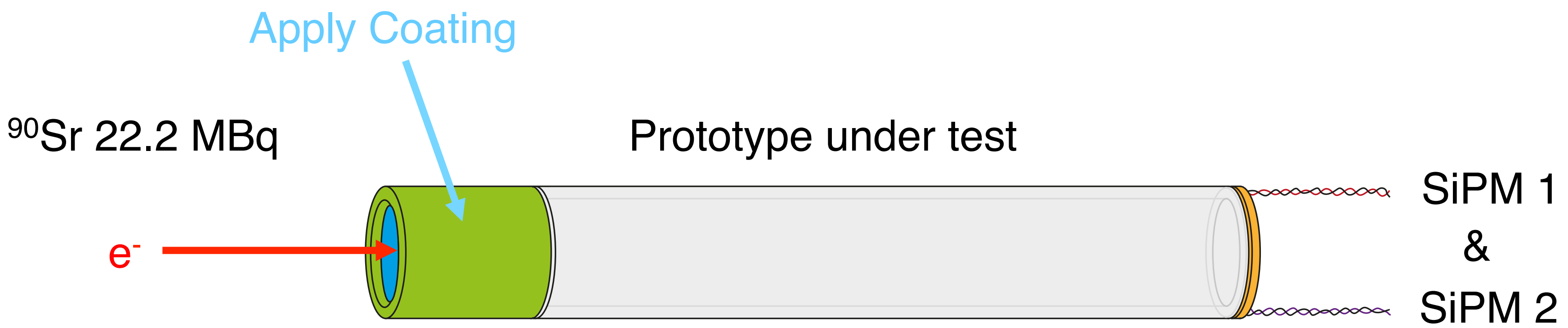

Maik Biroth, Institut für Kernphysik, Mainz, Germany
biroth@kph.uni-mainz.de

Benefit of Coating under ^{90}Sr Irradiation

Average intensity with ^{90}Sr is < 3 p.e. / 0.6 γ mm^{-2}
Discriminator cut off at 3 p.e. / $U_{TH} \geq$ 28mV
Measuring coincident event rate / dark counts subtracted

Prototype	Coating	Light Rate [s^{-1}]	Coating Benefit		Prototype Comparison
Segmented	-	61 ± 10	-	-	-
	Al foil	614 ± 18	10.08 ± 1.67	-	-
	Teflon	907 ± 22	14.88 ± 2.46	1.48 ± 0.06	-
Solid	-	480 ± 17	-	-	7.87 ± 1.32
	Al foil	1414 ± 31	2.95 ± 0.12	-	2.30 ± 0.08
	Teflon	2158 ± 43	4.50 ± 0.18	1.53 ± 0.05	2.38 ± 0.08

Al foil ➔ Teflon: +50%

Segemented ➔ Solid: +130%

Maik Biroth, Institut für Kernphysik, Mainz, Germany biroth@kph.uni-mainz.de

Modifications for Operation in the Cryostat

Cryostat insert

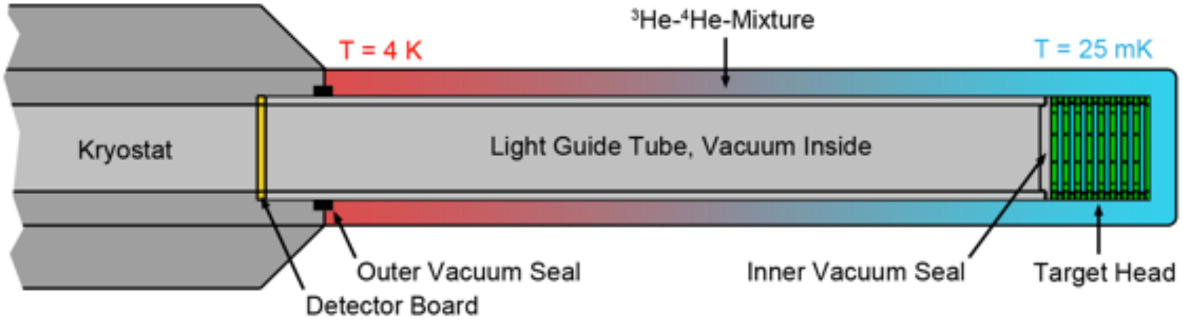

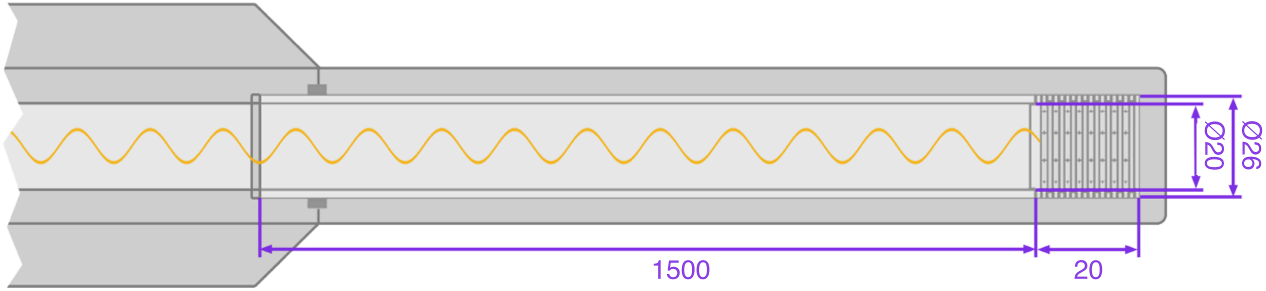

- Length of tube increased to 1.5m
  - \+ Operation of detectors at warmer regions
  - – Thermal short in the cryostat for high conductive materials
- Outer / inner vacuum seal
  - Not sealable with acrylic glass because of thermal contraction

Material Selection for the Light Guide Tube

Required features of the tube

- superfluid helium tightness
- high stability under thermal stress
- low thermal conductivity at low T
- good visible light transmission

Material options

- sapphire: high integral λ
- quartz: maximum λ at 7K
- glass: low and flat λ at low T

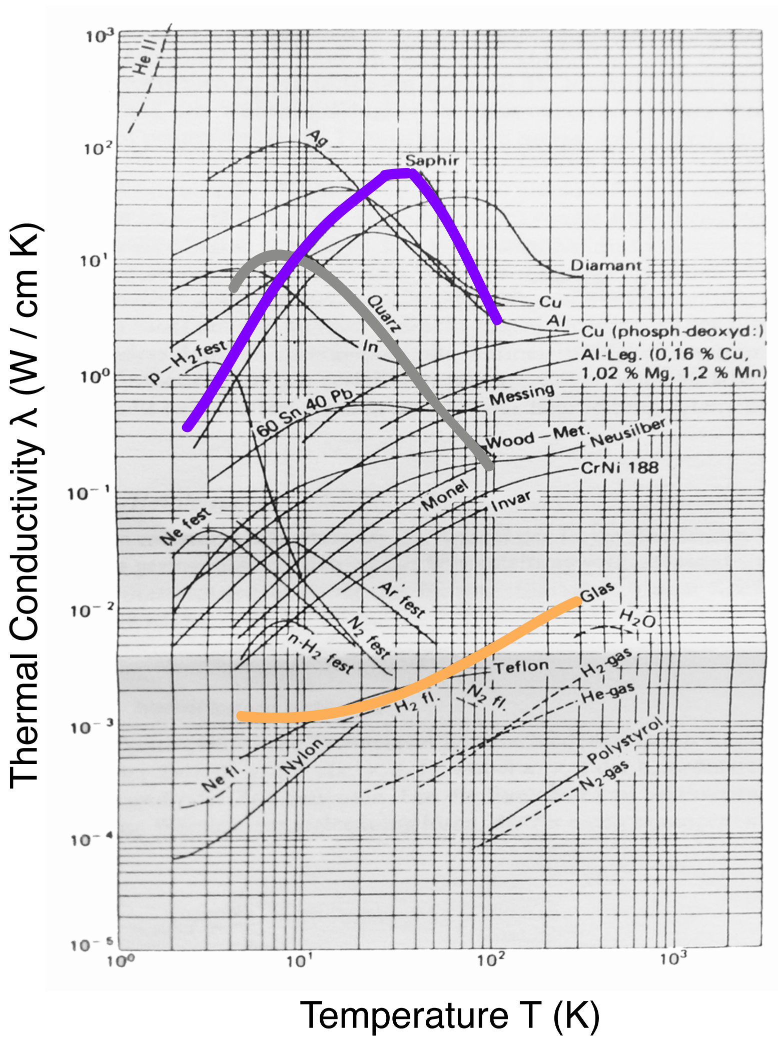

Maik Biroth, Institut für Kernphysik, Mainz, Germany
biroth@kph.uni-mainz.de

Stress Test of the Light Guide Tube and the Inner Vacuum Seal

Light guide and vacuum seal made from Borosilicate

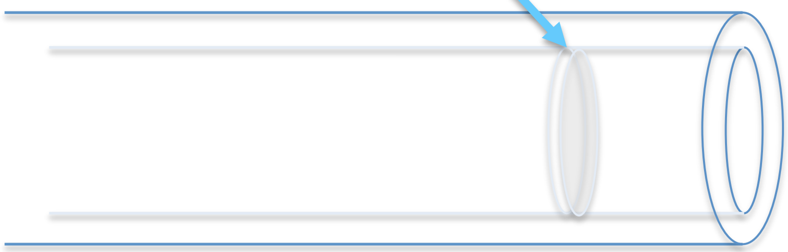

Sealing from outside with vapor-deposited copper and indium

Passed thermal and pressure strength test
Cooling down from 300 K to 77 K
at once and evacuating to $7 \cdot 10^{-10}$ mbar

Standard glass
flange for evacuation

Adhesion of the Parts with Divergent Coefficients of Thermal Expansion

Proceeding has to be different compared to room temperature

for example: optical grease freezes out

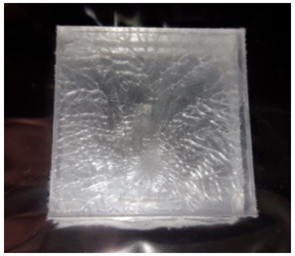

WLS Plastic ($78 \cdot 10^{-6}$ K^{-1})

Borosilicate ($3.3 \cdot 10^{-6}$ K^{-1})

Polystyrene scintillator ($70 \cdot 10^{-6}$ K^{-1}) and PMMA spacers ($70\text{-}77 \cdot 10^{-6}$ K^{-1})

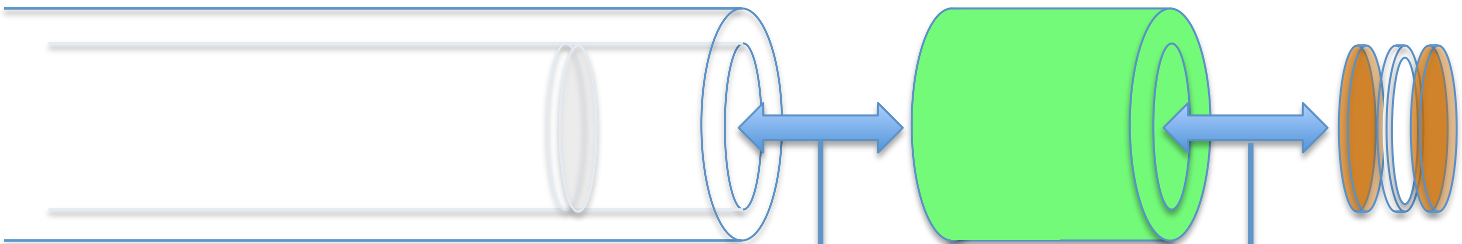

Epoxy Epo-Tek 301-2 ($61 \cdot 10^{-6}$ K^{-1})
High shear strength of
2000 psi / 140 kg cm^{-2}

Epoxy Epo-Tek 301-2
or silicone rubber
Elastosil RT 601
for exchangeable stack

Maik Biroth, Institut für Kernphysik, Mainz, Germany biroth@kph.uni-mainz.de

Cryogenic Operation of Optical Detectors

- Overview of detector types
- Testing SiPMs at cryogenic temperatures
- SiPM preamplifier design

Detectors Operational at Cryogenics

Required features of the detector

- High gain
- High rate capability
- Small surface mount type

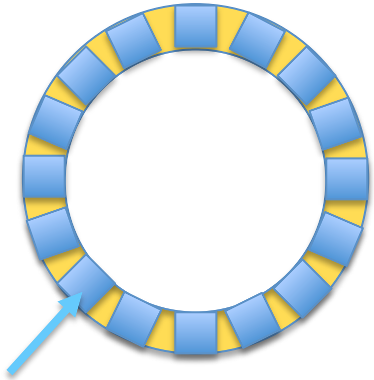

Mount devices on a PCB ring to cover the light guide

APD RMD AE228-4

- Gain 10^3 at V = 31V, T = 4K
- Special cryogenic type
- Expensive unique piece

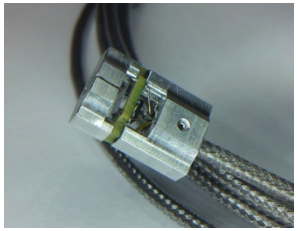

Custom SiPMs

- High gain $10^4 – 10^6$, good time resolution
- Cryogenic operation has to be proofed
- Unexpensive custom types

NbN SNSPD – Superconducting nanowire single-photon detectors

- High gain, good time resolution 60 ps
- Only operational at cryogenics
- In an experimental state

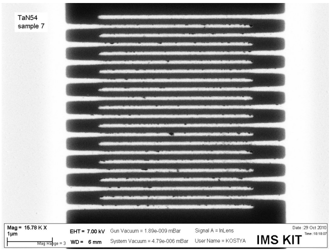

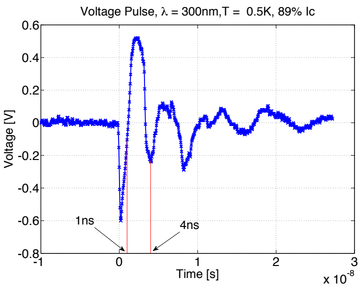

A. Aeschbacher, Superconducting Nanowire Single-Photon Detectors based on TaN Thin Films, Master Thesis, 2011

C. M. Natarajan et al. Superconducting nanowire single-photon detectors: physics and applications, Supercond. Sci. Technol. 25 (2012) 063001 (16pp)

Cryogenic Tests with SiPMs

Operation of many SiPMs
causes problems at cryogenics
after-pulse probability increases, quenching fails,…

New type of SiPM with high fill factor and quenching by potential walls

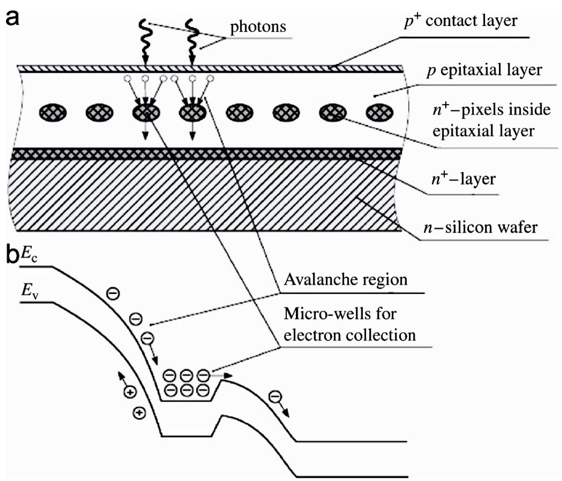

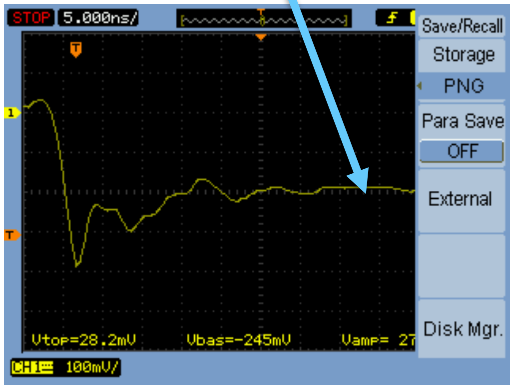

Hamamatsu S10362-11

MAPD-3N operational at liquid nitrogen temperature, but epoxy window cracked

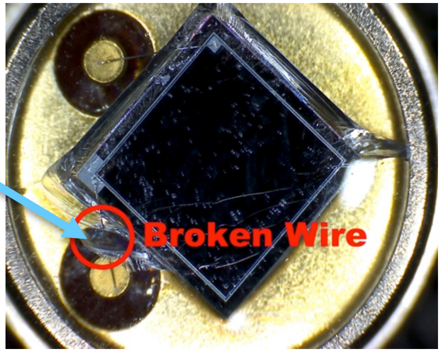

Zecotek MAPD White Paper, Zecotek Photonics, Richmond, Canada, 2011
Z. Sadygov et al. Performance of new Micro-pixel Avalanche Photodiodes from Zecotek. Nucl. Instrum. and Meth. A, 610:381–383, 2009

biroth@kph.uni-mainz.de

Modifications of a Custom MAPD-3N

- Epoxy cover was removed with acetone and chlorinated hydrocarbons
- New bonding wire connections were made

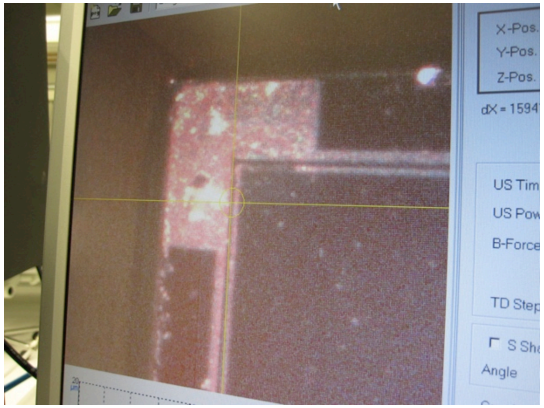

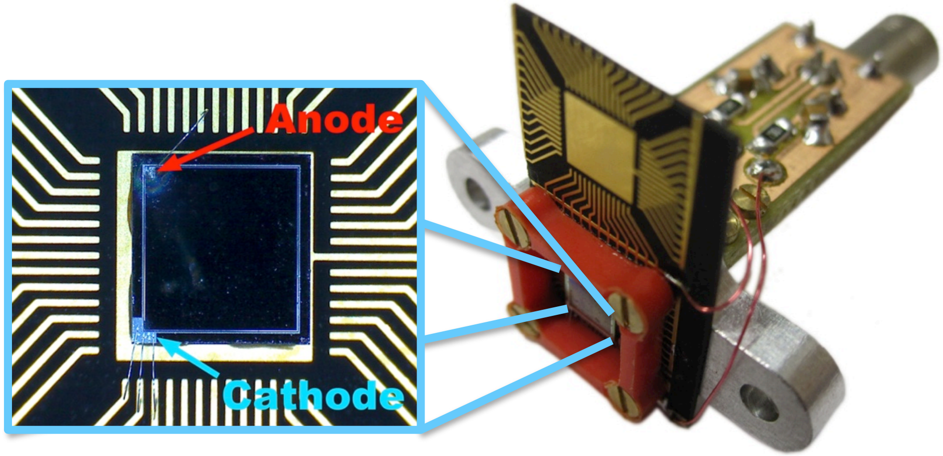

Thanks to Harald Deppe and the hole team of CSEE Electronics, GSI, Darmstadt, Germany

Maik Biroth, Institut für Kernphysik, Mainz, Germany
biroth@kph.uni-mainz.de

Setup for SiPM Characterization at Liquid Helium Temperatures

SiPM submerged in LHe,
Pre-amps outside the dewar

Measuring dark-counts
Discriminate the signal with darkened light guide

Testing the light response
Varying intensity by set the length of LED pulses

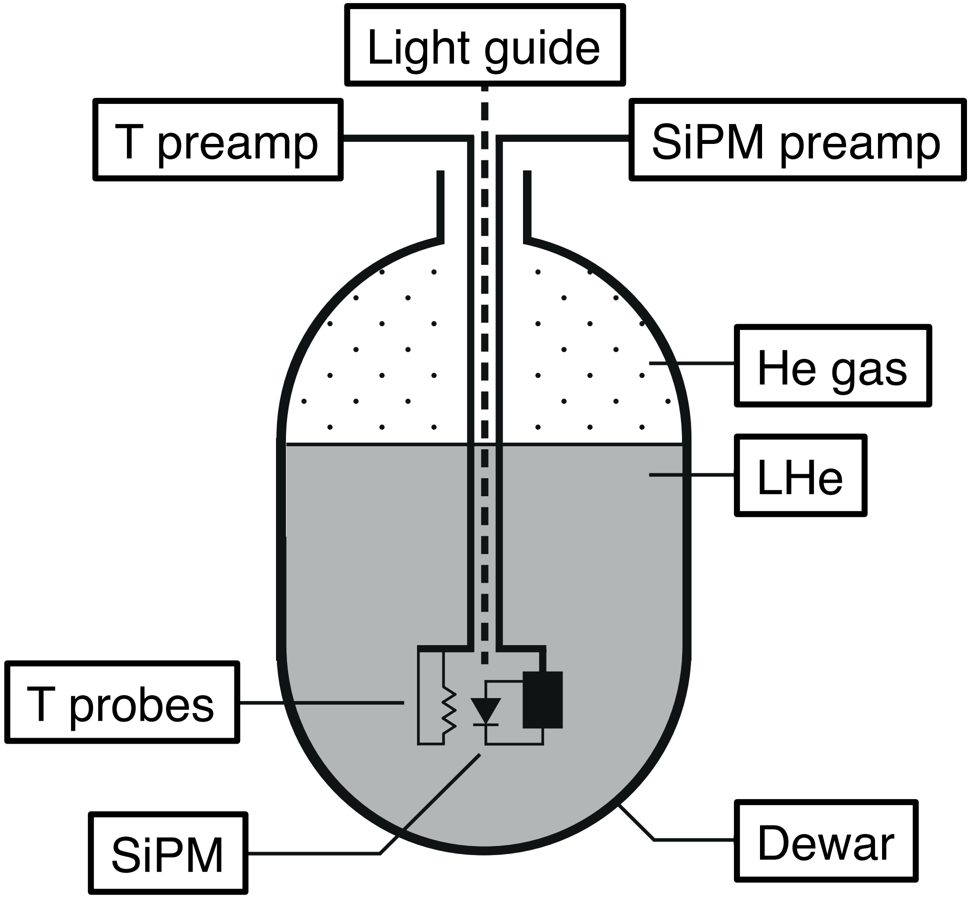

M. Biroth et al. Silicon photomultiplier properties at cryogenic temperatures
Nucl. Instr. and Meth. A 787 (2015) 68-71

SiPM Signal Shape at LHe

Rise time 10ns
Fall time 30ns
No change to RT

No after-pulses

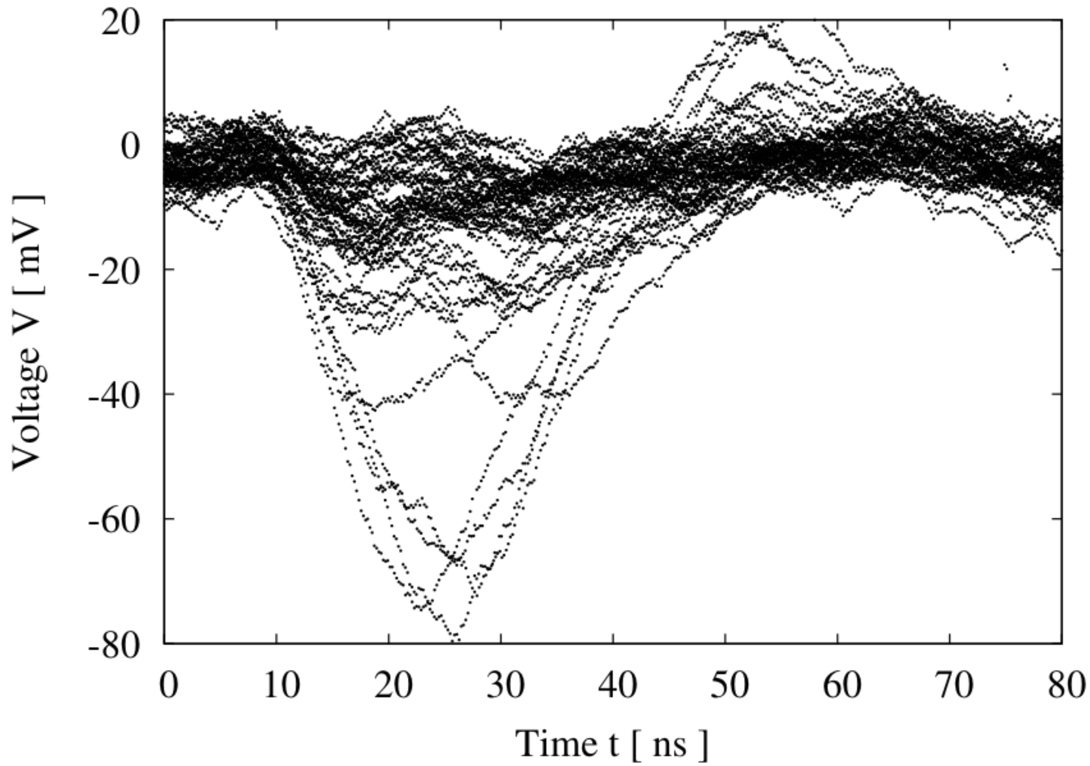

SiPM Dark-count Rate at LHe

Almost no dark-counts at LHe

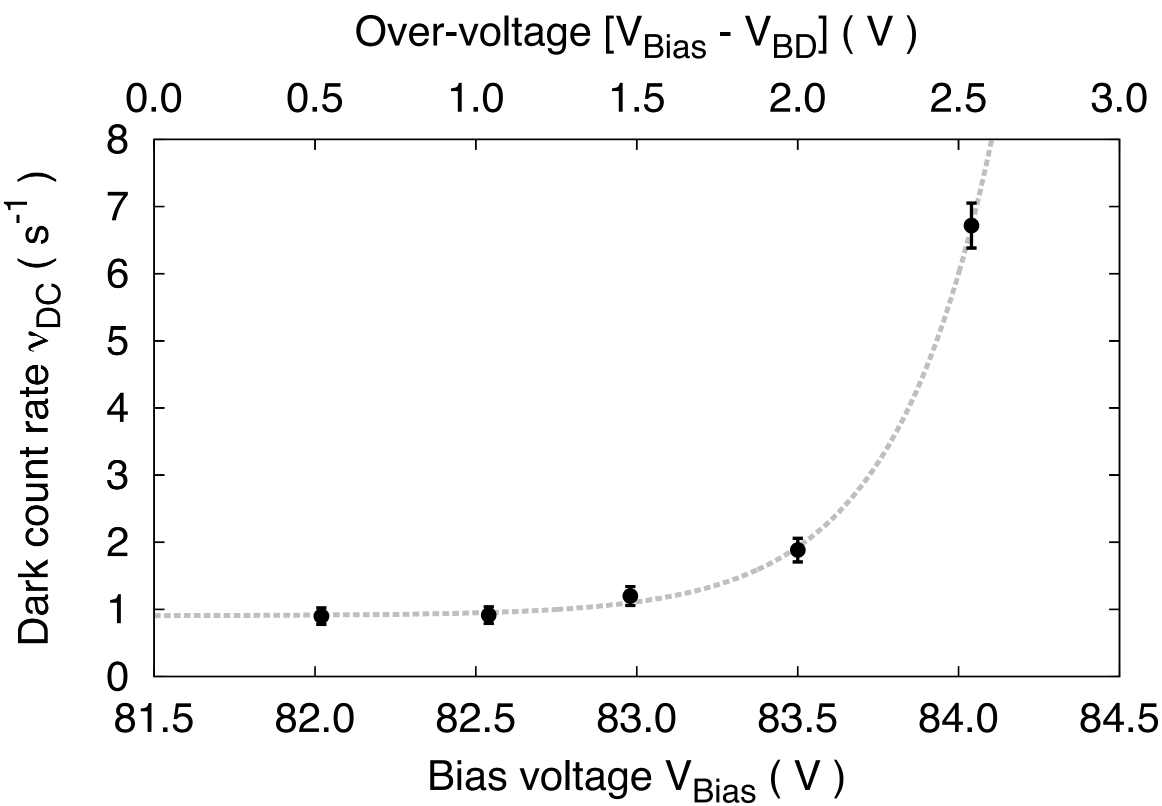

SiPM Signle-pixel Gain at LHe

Identical pixel-capacities at RT and LHe / over-voltage behavior

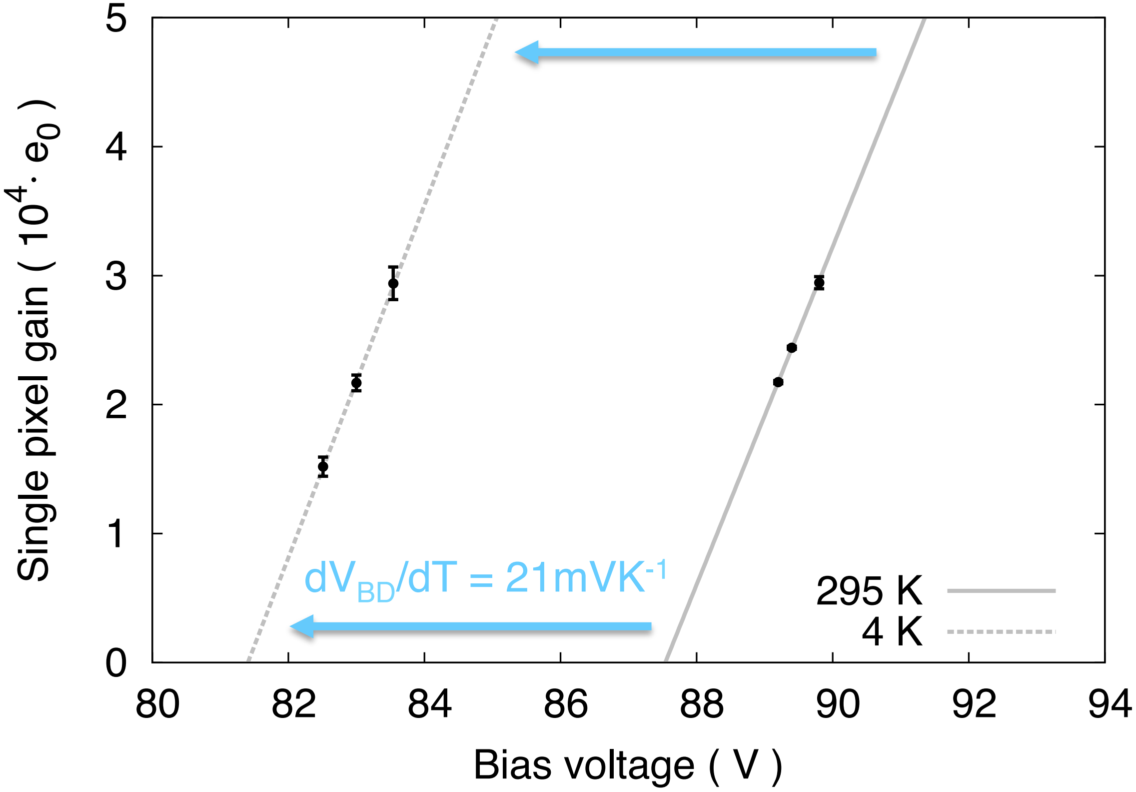

biroth@kph.uni-mainz.de

Test of the new MAPD-3N Types at Liquid Nitrogen Temperatures

MAPD-3NK0
135 kPx / 3.7x3.7 mm²
Pixel capacity 6.3 fC

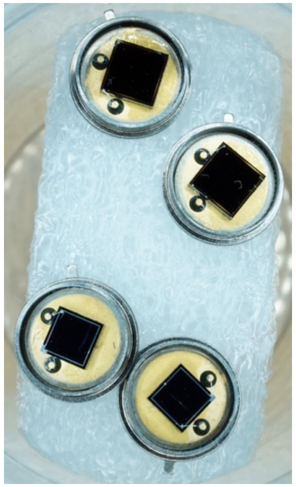

MAPD-3N1P
135 kPx / 3.0x3.0 mm²
Pixel capacity 4.3 fC

Gain of both SiPMs depends linear from the over-voltage at LN temperatures
(example plot at 100K)

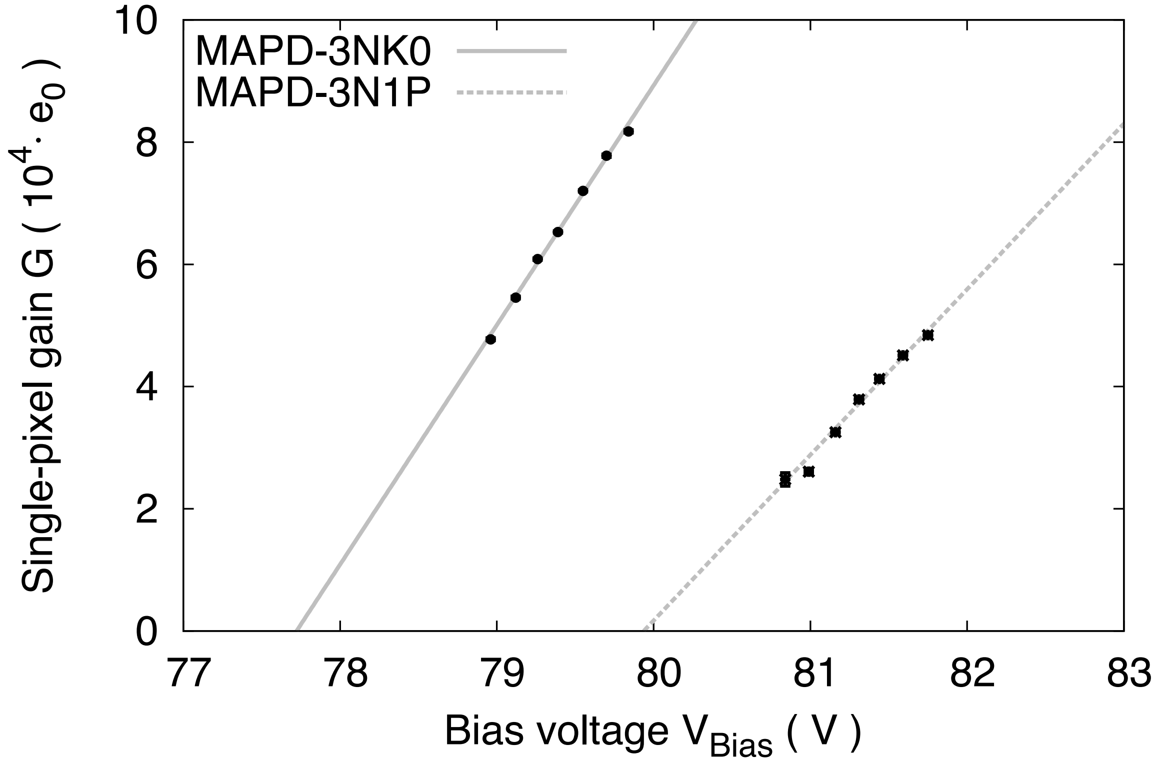

Characterization at liquid helium follows…

Maik Biroth, Institut für Kernphysik, Mainz, Germany
biroth@kph.uni-mainz.de

Low-noise 4 Wire SiPM Pre-amplifier with AC/DC Measurement

4 wire detector board and preamplifier

DC gain: 10 MVA^{-1} (1 stage) / resolution < 100 pA

AC gain: 100 kVA^{-1} (2 stages) / bandwidth 200 MHz

2.5 m distance from SiPM to amplifier

Required features

- high bandwidth
- high noise-immunity
- high tolerance of stray capacities

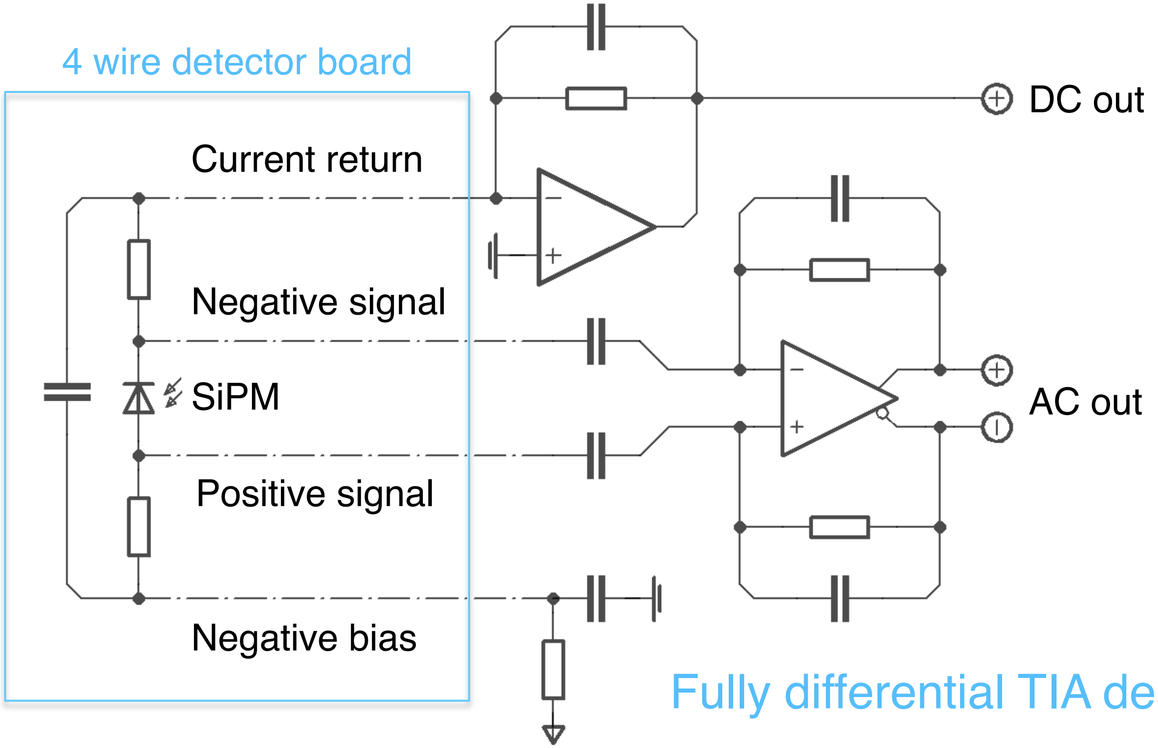

Symmetrical low-pass filter placed directly at the SiPM

Fully differential TIA design

M. Biroth et al. A low-noise and fast pre-amplifier and readout system for SiPMs Nucl. Instr. and Meth. A 787 (2015) 185-188

SiPM Preamplifier Upgrade with Increased AC Gain

Increased AC gain to 100kΩ
(example charge spectrum for MAPD-3NK0 at 100K, Gain $6.6 \cdot 10^4$ e_0)

Single-pixel peaks are good separated

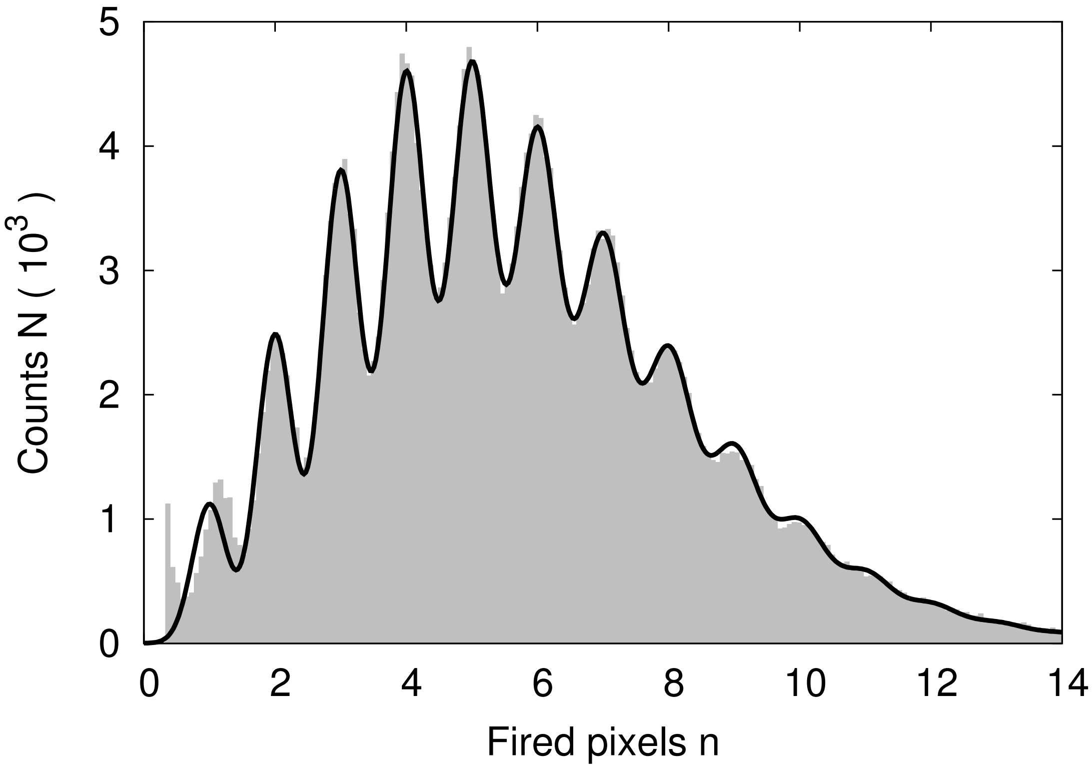

Maik Biroth, Institut für Kernphysik, Mainz, Germany
biroth@kph.uni-mainz.de

SiPM Preamplifier Upgrade with DC measurement

SiPM light response acquired by high precision DC measurement (resolution 100pA)

(example plot for MAPD-3NK0 at 95K)

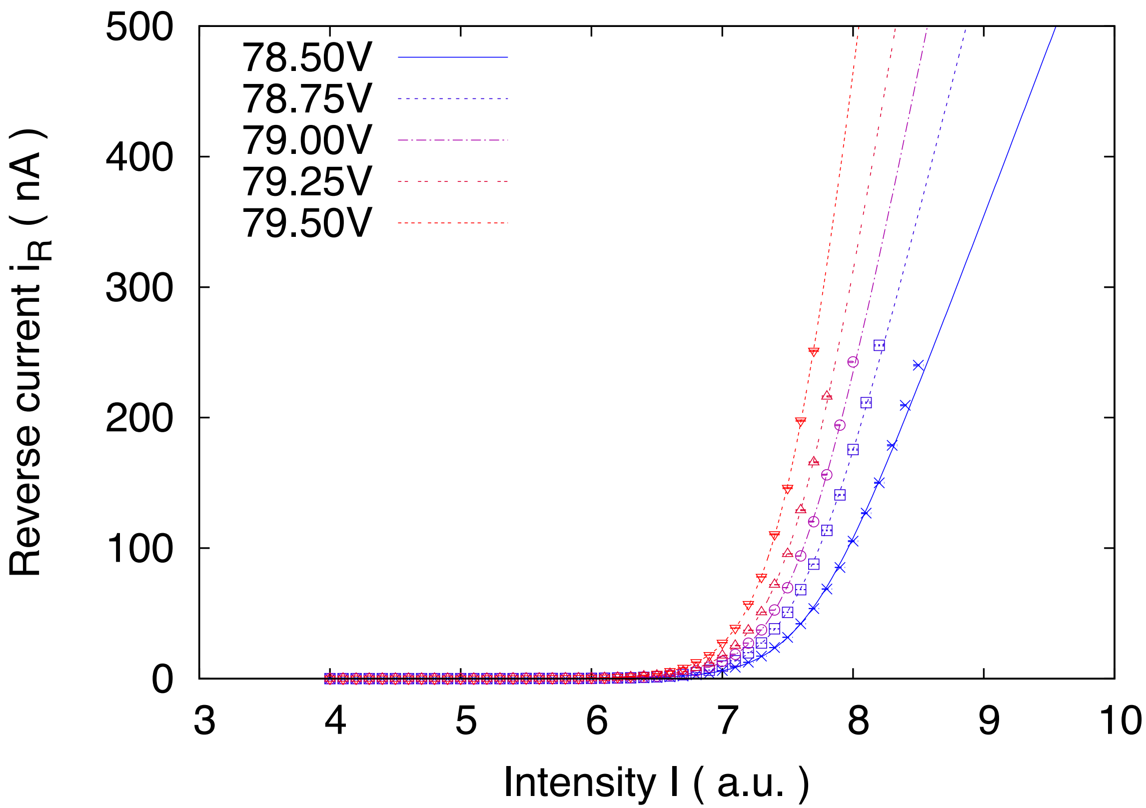

DC is useful for bias voltage setting and rate monitoring

Conclusion and Outlook

Hardware

- ✓ Design for the Mainz APPT was found, capable to separate protons from el-mag. background
- ✓ Light guide from borosilicate can be sealed and has good optical properties
  - Stability tests of adhesive surface between light guide and target head

Electronics

- ✓ Pre-amplifier was upgraded with DC measurement
- ✓ MAPD-3N was operated successfully at LHe
- ✓ New MAPD-3N types were operated at LN
  - Ongoing LHe test

Potential Experiments Which Will Profit of an Active Polarized Proton Target

Every high precision double-polarized measurement of the proton at the pion production threshold can profit

- Real Compton Scattering
- Test of the GDH sum rule

Real Compton Scattering on the Proton

Double-polarization experiment

- Polarized proton target (longitudinal, transversal)
- Polarized photon beam (circular, linear)

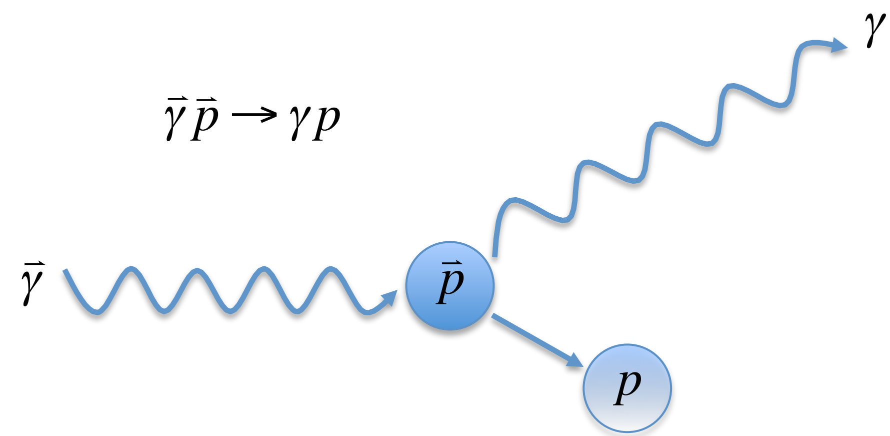

Nucleon spin precesses
as an answer to the
photon spin

Spin-polarizabilities γ_{E1E1}, γ_{M1M1}, γ_{E1M2}, γ_{M1E2} describe nucleon spin-flip at $O(\omega^3)$ of scattering amplitude in terms of the photon energy

$$\mathrm{H}_{eff}^{(3)} = -2\pi \cdot \left[\gamma_{E_1 \to E_1} \cdot \vec{\sigma} \cdot \left(\vec{E} \times \dot{\vec{E}} \right) + \gamma_{M_1 \to M_1} \cdot \vec{\sigma} \cdot \left(\vec{H} \times \dot{\vec{H}} \right) + 2 \cdot \gamma_{E_1 \to M_2} \cdot \sigma_i \cdot H_{i,j} \cdot E_j - 2 \cdot \gamma_{M_1 \to E_2} \cdot \sigma_i \cdot E_{i,j} \cdot H_j \right]$$

Maik Biroth, Institut für Kernphysik, Mainz, Germany biroth@kph.uni-mainz.de

Data Situation of the Spin-Polarizabilities

New experimental data for γ_{E1E1}, γ_{M1M1}, γ_{E1M2}, γ_{M1E2}

Compared to the forward γ_0 and backward γ_π spin-polarizabilities, increased accuracy can be reached

$$\gamma_0 = -\gamma_{E_1 \to E_1} - \gamma_{M_1 \to M_1} - \gamma_{E_1 \to M_2} - \gamma_{M_1 \to E_2} \qquad \gamma_\pi = -\gamma_{E_1 \to E_1} + \gamma_{M_1 \to M_1} - \gamma_{E_1 \to M_2} + \gamma_{M_1 \to E_2}$$

	ChPT			LI ChPT		SSE	Fixed-t Dispersion Analysis				Experiment
	$O(p^3)$	$O(p^4)$	$O(p^4)$	$O(p^3)$	$O(p^4)$		BGLMN	HDPV	KS	DPV	
γ_{E1E1}	-5.7	-1.4	-1.8	-3.2	-2.8	-5.7	-3.4	-4.3	-5.0	-4.3	-3.5 ± 1.2
γ_{M1M1}	-1.1	3.3	2.9	-1.4	-3.1	3.1	2.7	2.9	3.4	2.9	3.16 ± 0.85
γ_{E1M2}	1.1	0.2	.7	.7	.8	.98	0.3	-0.01	-1.8	0	-0.7 ± 1.2
γ_{M1E2}	1.1	1.8	1.8	.7	.3	.98	1.9	2.1	1.1	2.1	1.99 ± 0.29
γ_0	4.6	-3.9	-3.6	3.1	4.8	.64	-1.5	-.7	2.3	-.7	-1.01 ± 0.08 ± 0.10
γ_π	4.6	6.3	5.8	1.8	-.8	8.8	7.7	9.3	11.3	9.3	8.0 ± 1.8

All values are in units of 10^{-4} fm^4

Pion-pole contribution was subtracted of γ_π

Table: R. Miskimen, Measuring Proton Spin-Polarizabilities with the Crystal Ball, A2-Collaboration Meeting 2014

Data: P. P. Martel et al. Measurements of Double-Polarized Compton Scattering Asymmetries and Extraction of the Proton Spin Polarizabilities, PRL 114, 112501 (2015)

Maik Biroth, Institut für Kernphysik, Mainz, Germany
biroth@kph.uni-mainz.de

The RCS Polarization Observables

Polarization observables Σ_{2x}, Σ_{2z}, Σ_3 are asymmetries to different spin settings, sensitive to the spin-polarizabilities

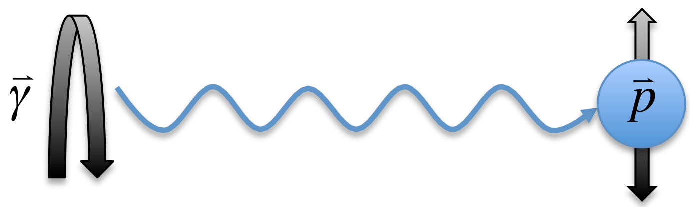

$$\Sigma_{2x} = \frac{\sigma^{\uparrow} - \sigma^{\downarrow}}{\sigma^{\uparrow} + \sigma^{\downarrow}}$$

Sensititve to γ_{E1E1}

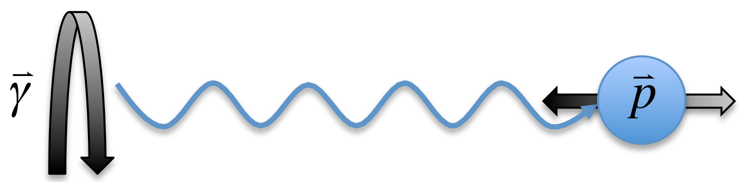

$$\Sigma_{2z} = \frac{\sigma^{\rightarrow} - \sigma^{\leftarrow}}{\sigma^{\rightarrow} + \sigma^{\leftarrow}}$$

Sensititve to γ_{M1M1}

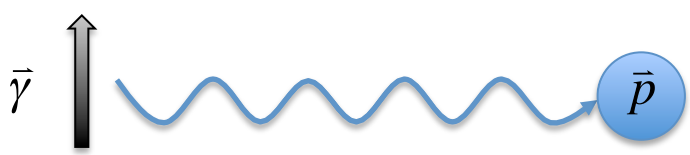

$$\Sigma_{3} = \frac{\sigma^{\parallel} - \sigma^{\perp}}{\sigma^{\parallel} + \sigma^{\perp}}$$

Sensititve to γ_{M1M1}, γ_{M1E2}

Maik Biroth, Institut für Kernphysik, Mainz, Germany biroth@kph.uni-mainz.de

Background Reactions and Suppression

Background caused by π^0 production

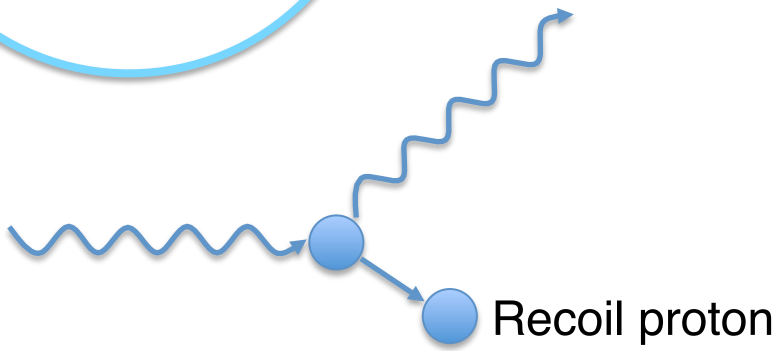

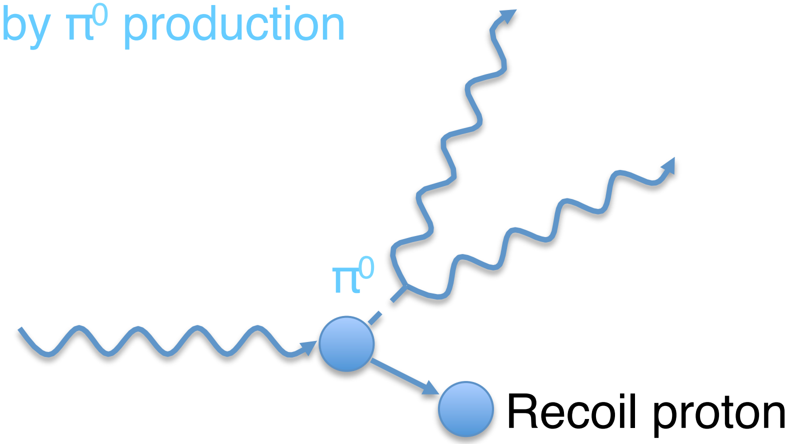

Background caused by coherent scattering

Incoherent scattering

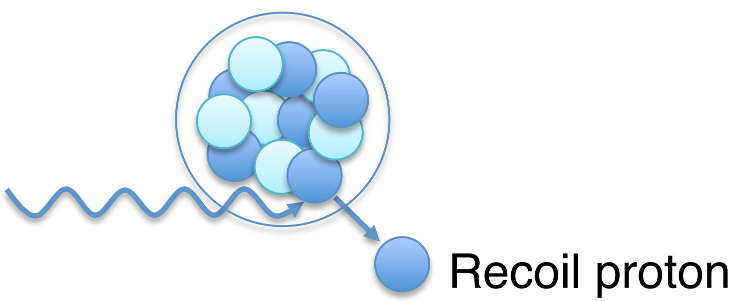

Coherent scattering
on ^{12}C or heavy nuclei

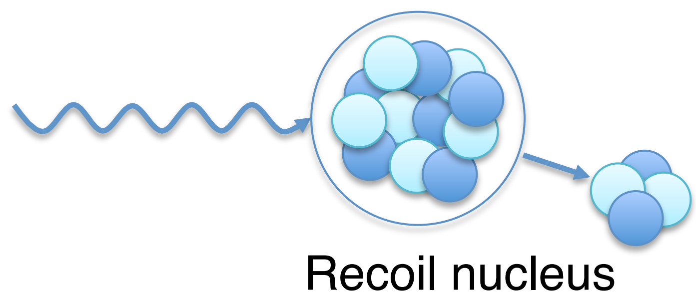

Maik Biroth, Institut für Kernphysik, Mainz, Germany
biroth@kph.uni-mainz.de

The Gerasimov-Drell-Hearn (GDH) Sum Rule

Linking between helicity dependent photo-absorption cross section and anomalous magnetic moment κ of longitudinal polarized nucleons

$$I_{GDH} := \int_{m_\pi}^{\infty} dE_\gamma \cdot \frac{\sigma_{3/2}^{\leftarrow} - \sigma_{1/2}^{\rightarrow}}{E_\gamma} = \frac{2\pi^2\alpha}{M_N^2} \cdot \kappa_N^2$$

At low energies single-pion production is dominant

$$\vec{\gamma}\vec{p} \rightarrow \pi N$$

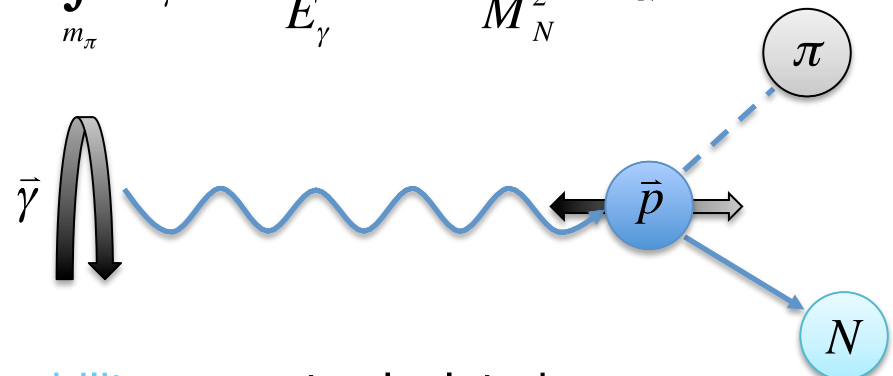

Furthermore the forward spin polarizability can get calculated from the total cross section difference

$$\gamma_0 = \frac{1}{4\pi^2} \int_{m_\pi}^{\infty} dE_\gamma \cdot \frac{\sigma_{3/2}^{\leftarrow} - \sigma_{1/2}^{\rightarrow}}{E_\gamma^3} \equiv -\gamma_{E_1 \rightarrow E_1} - \gamma_{M_1 \rightarrow M_1} - \gamma_{E_1 \rightarrow M_2} - \gamma_{M_1 \rightarrow E_2}$$

Pion Production at the Threshold

Missing data points for $\vec{\gamma}\vec{p} \rightarrow \pi^{+} n$
140 – 200 MeV where E_{0+} is dominant

E_γ (GeV)	Source	I_{GDH} (mb)
0.14 – 0.20	MAID SAID	-27.5 -28
0.20 – 2.90	Exp. (MAMI + ELSA)	253.5±5±12
2.90 – ∞	Simula et al. Bianchi and Thomas	-13 -14
Total		211.5-213
GDH sum rule value		205

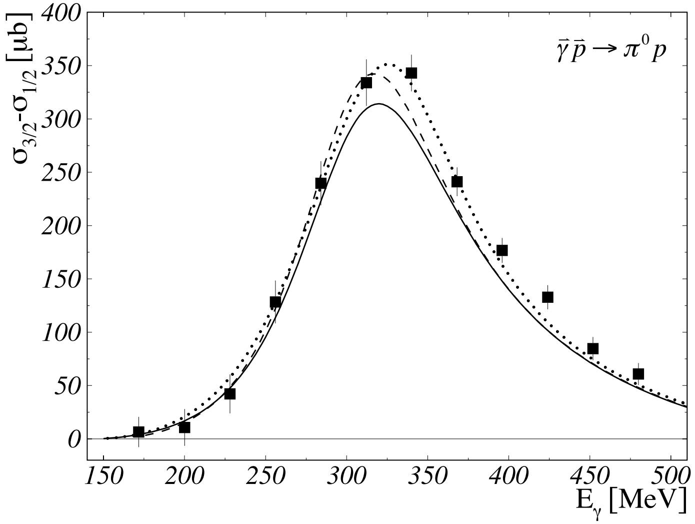

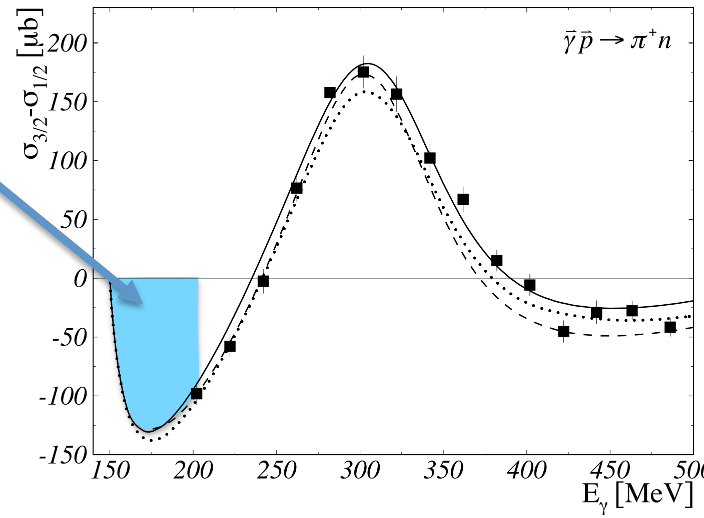

Table: A. Thomas, The Gerasimov-Dree-Hearn sum rule at MAMI, Eur. Phys. J. A 28, s01, 161–171 (2006)
Plots: I. Preobrajenski, Untersuchung der Helizitätsabhängigkeit der Einpionproduktion am Proton, PhD Thesis 2001